J Opt (December 2020) 49(4):427–432
https://doi.org/10.1007/s12596-020-00642-2

RESEARCH ARTICLE

Bandwidth-tunable optical filter based on microring resonator and MZI with Fano resonance

Xia Li[1] · Chen Shen[1] · Xiaohan Yu[1] · Yanqiong Zhang[1] · Chao Chen[1] · Xiaoxu Zhang[1]

Received: 12 January 2018 / Accepted: 1 August 2020 / Published online: 30 September 2020

Abstract A bandwidth-tunable optical filter is fabricated by combining Mach–Zehnder interferometer (MZI) and microring resonator. Both bandwidth red-shift and blue-shift are observed in the experiment. The bandwidth can be tuned from 0.46 to 3.09 nm by controlling two phase shifters. The device also shows an extinction ratio higher than 25 dB. Potential applications are integrated optical signal processing such as reconfigurable filtering and channel selecting in wavelength division multiplexer.

Keywords Filter · Bandwidth tunable · Silicon · Ring resonator · Wavelength division multiplexer

Introduction

Wavelength division multiplexing systems play a more and more important role in the next generation telecom networks [1]. In this scenario, the bandwidth-tunable optical filters are one of the basic components. They can be used in the implementation of the gridless paradigm in wavelength division multiplexing systems. To obtain such bandwidth tunability, many solutions have been researched. The recent development of optical ring becomes more and more attractive due to a variety of functionalities such as compact structure, high Q-factor and compatible with mature silicon microelectronics [2–4]. Taking the huge advantages of microring resonators, lots of devices have been used in high sensitive sensors, all optical switching and reconfigurable add–drop filters [5–7]. In previous works, many bandwidth-tunable devices have been fabricated utilizing the characteristic of symmetric resonance in microring resonators (MRRs) [8–12]. For example, one is the filter based on a single microring resonator. Its coupling coefficient of the resonator is tuned by micro-electronic-mechanical-system. However, a high actuation voltage of nearly 40 V should be applied to realize the MEMS tunability [5]. Another one is also a filter based on a single microring resonator [13]. Its coupling coefficient of the resonator is tuned by the thermo-optic phase shifters. The disadvantage of this filter is that it offers limited bandwidth variation range and poor off-band rejection. There is also a filter combining a MZI and ring resonator, the ring resonators are embedded in the MZI arms, and its bandwidth tuning is limited due to in-band ripples and insertion loss [14].

In this letter, we demonstrate a bandwidth-tunable optical filter based on the ring resonators and MZI with Fano resonance. It consists of two single MRRs and a MZI structure constituted by two 1×2 multi-mode interferences (MMI). The coupling coefficients of the two single MRRs are both tuned by the thermo-optic phase shifters. In this new design, the two MRRs, controlled by two TiN heaters, are available to produce an extra phase to break the symmetric Lorentz shape of normal MRRs. Fano resonance can be observed through the superposition of two asymmetric Lorentz shapes, and the 3 dB-passband was obviously broadened. By means of thermo-optic (TO) properties of silicon, the bandwidth ranges from 0.46 to 3.09 nm, wider than that of previous devices. The extinction ratio of output port is more than 25 dB, and the free spectrum range (FSR) is 9.2 nm, which is suitable for the transmission in optoelectronic integrated circuits. It is known that through port 3 dB, bandwidth is an important

✉ Xia Li
21131062@zju.edu.cn

[1] Department of Information Science and Electronics Engineering, Zhejiang Gongshang University, Hangzhou 310018, China

parameter which may require tuning in optical waveform generation [10, 15].

Theoretical analysis and device structure

Many previous models and theories show that the coupling coefficient between microring and straight waveguide can determine the 3 dB bandwidth of the filters [13]. So the passband of filters can be tuned by changing this equivalent coefficient [12, 14]. The 3 dB bandwidth of the filter is decided by the coupling coefficient between microring and U-bend arm; therefore, we can alter this equivalent coefficient so as to tune the passband of filters. Figure 1 shows the theoretical model which we construct. We derive the following expression by the transfer matrix method.

$$I_0 = |E_0|^2 = \left| \frac{\alpha^{1/2} k^2 e^{-i(\theta/2+\pi)} + \gamma t^2 e^{-i\theta_1} + \alpha\gamma e^{-i(\theta+\theta_1+\pi)}}{1 - \alpha t^2 e^{-i\theta} - \alpha^{1/2}\gamma k^2 e^{-i(\theta_1+\theta/2+\pi)}} \right|^2 \quad (1)$$

where t, k are the transmission and the coupling coefficients, respectively, $t = t_1 = t_2$, $k = k_1 = k_2$.The insertion losses of the couplers are assumed to be zero in the calculation, $k^2 + t^2 = 1$. And the parameters α and γ represent the transmission loss coefficients in the whole microring and U-bend waveguide, respectively. While the parameters θ_0 and θ_1 are the changes of phase during the transmission in both two pathways.

There are two coupling resonant cavities, namely MRR and racetrack-like resonator formed by a semi-ring and the U-bend waveguide, as shown in the proposed device. The Fano resonance originates from interference between a discrete state and a continuum state [16]. The term $1 - \alpha t^2 e^{-i\theta}$ of the denominator in Eq. (1) is the resonance of the MRR, which can be regarded as discrete resonant states; the term $\left|1 - \alpha^{1/2}\gamma k^2 e^{-i(\theta_1+\theta/2+\pi)}\right| \approx 1$ (assuming that the coupling coefficient is small and the cavity length is long) is the resonance of the racetrack-like resonator. There are three paths of the modes propagating from the input to the output. The first one is the mode propagating from the input to the output via MRR. The second one is the mode propagating from the input to the output via U-bend waveguide. The third one is the mode propagating from the input to the output via the modes interaction between the MRR and the U-bend waveguides. The three paths can be represented by

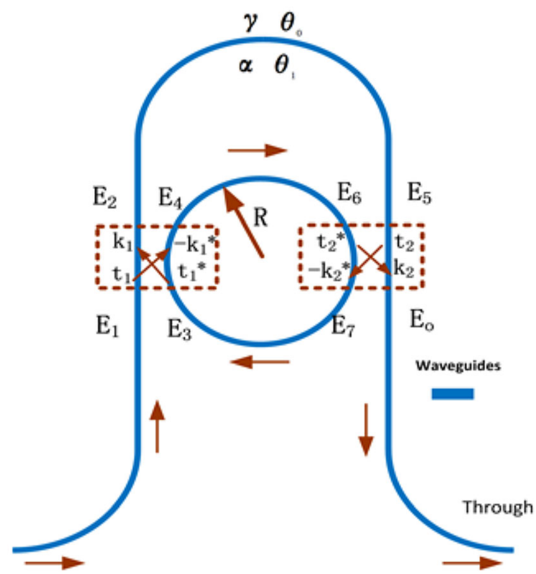

Fig. 1 Schematic of single ring resonator with the U-bend waveguide

$\alpha^{1/2}k^2e^{-i(\theta/2+\pi)}$, $\gamma t^2 e^{-i\theta_1}$ and $\alpha\gamma e^{-i(\theta+\theta_1+\pi)}$ of the numerator in Eq. (1), respectively. When $\alpha = \gamma = 0.95 \approx 1$, this means the U-bend approaches lossless, then the resonant system is equivalent to the notch filter, of which the transmission spectrum is shown in Fig. 2a. When $\alpha = 0.95$, $\gamma = 0$, this means the light signal cannot transmit through the U-bend waveguide, then the resonant system can be equivalent to the add-drop filter, whose transmission spectrum is in contrast to Fig. 2a. As is known to all, the two transmission spectra are both symmetrical Lorenz shape. When $\alpha = 0.95$, $0 < \gamma < 1$ $(\gamma = 0.9)$, the transmission spectrum will be a Fano resonance, as is shown in Fig. 2b. The extinction ratio gets smaller as k grows down. According to Eq. (1), as k grows down, the denominator gets bigger, the numerator gets smaller, and then the output power $|E_0|^2$ becomes smaller. The extinction ratio will be along with becoming smaller.

To widen the tunable bandwidth, the transmissions of two single ring resonators are combined together in the MZI structure, as we can see from Fig. 3. One microheater is placed over the U-bend arm to change φ_1. Another microheater placed over the ring is proposed to change φ_2. The output port will combine the two resonance waves, and then, it will generate the Fano resonance as long as the two waves are not exactly the same. The total transmission can be obtained by transfer matrix method as follows:

$$I_0 = |T_1 + T_2|^2 = \left| \frac{\alpha^{1/2} k_3^2 e^{-i(\theta/2+\pi)} + \gamma t_3^2 e^{-i\theta_1} + \alpha\gamma e^{-i(\theta+\theta_1+\pi)}}{1 - \alpha t^2 e^{-i\theta} - \alpha^{1/2}\gamma k_3^2 e^{-i(\theta_1+\theta/2+\pi)}} + \frac{\alpha^{1/2} k_4^2 e^{-i(\theta/2+\pi)} + \gamma t_4^2 e^{-i\theta_1} + \alpha\gamma e^{-i(\theta+\theta_1+\pi)}}{1 - \alpha t^2 e^{-i\theta} - \alpha^{1/2}\gamma k_4^2 e^{-i(\theta_1+\theta/2+\pi)}} \right|^2 \quad (2)$$

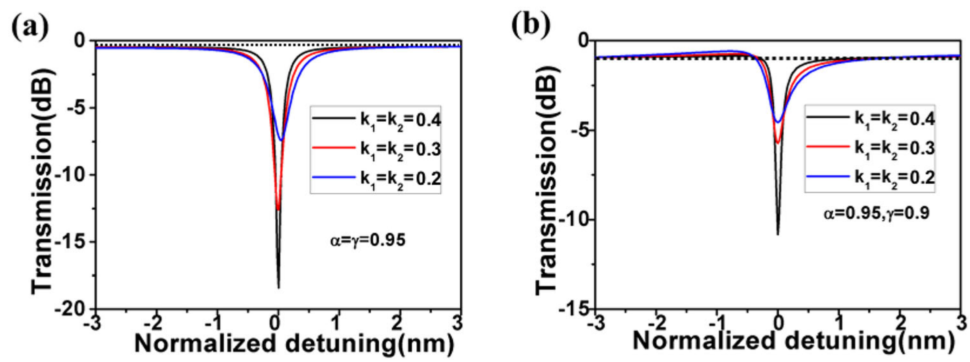

Fig. 2 Simulated transmission spectra of single MRR **a** with same amplitude attenuation factors **b** with different amplitude attenuation factors

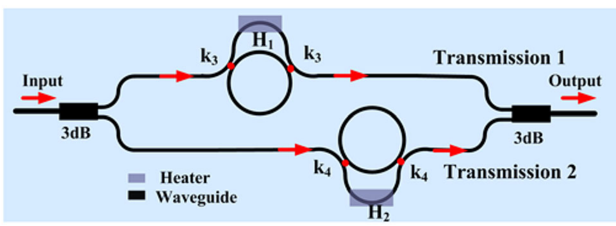

Fig. 3 Schematic of the tunable bandwidth filter with beam combiner

where t_i, k_i (i = 3,4) are the transmission and the coupling coefficients of two MRRs, respectively. T1 and T2 mean transmission 1 and transmission 2, respectively. The other parameters are the same with the single MRR. Figure 4 exhibits the principle of our device: the MRR_1 and MRR_2 in Fig. 3 separately propagate the coherent wave with different coupling coefficient $k_3 = 0.1$ and $k_4 = 0.4$. Although in each channel there is a symmetric Lorentz line figured by transmission 1 and transmission 2, the final transmission is an asymmetric Fano-resonance waveform. The reason is that the resonant points of the two MRRs are different. Then, the interfering between two different Lorentz shapes will break the balance of themselves. As we can see from Fig. 4b, the phase shift of the two MRRs are symmetric, while the symmetry of the phase shift in the total transmission is broken. And the total 3 dB bandwidth of final output is wider than that of single MRR and the extinction ratio is much larger. We also obtain that the total waveform broaden toward the smaller extinction ratio of transmission 1.

The reason why we set $k_3 = 0.1$ and $k_4 = 0.4$ is that the bandwidth of the optical filter is the largest under this condition when the heaters have not been applied the electric power. The radii of the two rings are both 10 μm, and the length of U-bend arm is 30 μm, more than half of the perimeter of MRR. The parameter α equals 0.9928 and γ equals 0.9. After calculation, it shows that the larger difference between k_1 and k_2 is, the wider the bandwidth becomes. By the limit of linewidth in manufacturing crafts, the coupling coefficient cannot exceed over 0.405 with above conditions, so we set $k_3 = 0.1$ and $k_4 = 0.4$.

The rib Si waveguides with a cross section of 450 nm × 220 nm and a 60 nm-thick-slab are employed. The coupling coefficient of k_3 and k_4 is designed to be 0.1 and 0.4, as mentioned above. The coupling coefficients are decided by the gaps between the bus waveguides and the ring waveguides. The relationship between them can be calculated by using the finite-difference time-domain

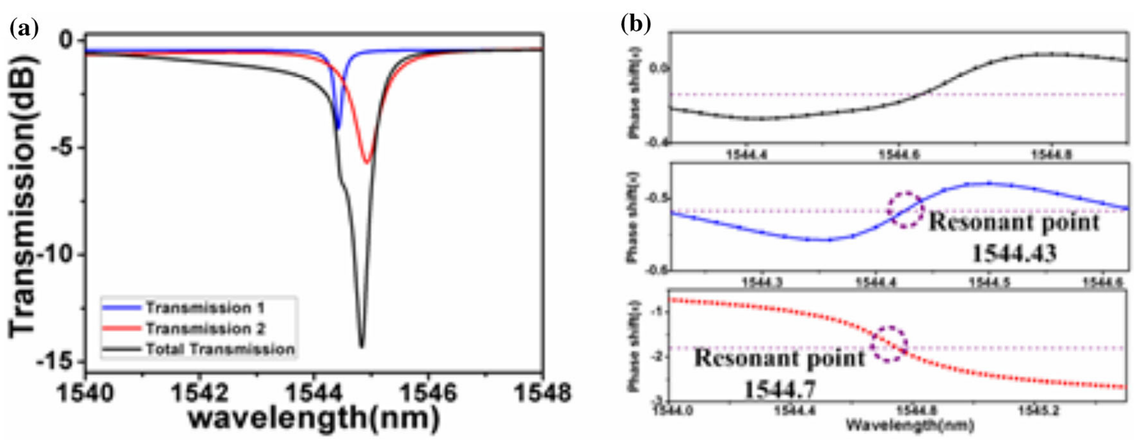

Fig. 4 **a** Transmissions of the two MRRs, as well as total transmission of the microring-MZI filter **b** phase shift of the two MRRs, as well as total phase shift of the microring-MZI filter. Here, parameters α = γ=0.95, $k_3 = 0.1$ and $k_4 = 0.4$

method. According to the relationship, the gaps are chosen to be 400 nm and 180 nm.

The device is fabricated on an 8-inch silicon-on-insulator (SOI) wafer with 220-nm-thick top Si layer and 2-μm-thick dioxide layer, and 248-nm-deep UV photolithography is used to define the device pattern. Grating couplers are integrated to couple light into and out of the device. The SiO_2 layer is deposited on the Si core layer, and then, the TiN heater is sputtered on the SiO_2 layer. Figure 5 is optical micrograph of the filter.

Experimental results and simulation comparison

First, the spectrum of single MRR is measured by applying different voltage on the heaters as shown in Fig. 6. The linear fit line of the phase shifts illustrates that it approximately increases linearly with the increase in the applied electric power on the heater. The 3 dB bandwidth becomes wider. Applying voltage on the heaters will lead the center wavelength shift (< 0.4 nm) [13]. In the future work, we will do some work to prevent the wavelength shift.

Then, the spectra of the bandwidth-tunable optical filter are measured. Figure 7 is the spectrum of the filter without applying the electric power. The red circle note and the blue circle note represent different MRR. We can see that the resonant wavelengths of the two MRRs are different. When applying different electric power on the heaters of two U-bend waveguides, the resonant wavelengths will both shift and close to each other. Then, the two transmissions will be combined together which will lead to the change of 3 dB bandwidth. The resonant wavelengths in the same MRR are not identical, as shown in Fig. 7. It is because that the coupling coefficient between the bus waveguide and the ring is wavelength related. It is not identical in different resonant wavelength when the critical coupling occurs. The different resonant wavelength will lead different Fano resonance. What we choose to expose in the paper is the largest bandwidth with Fano resonance. If we adjust the voltage adequately, it will reach the largest bandwidth in every resonant wavelength.

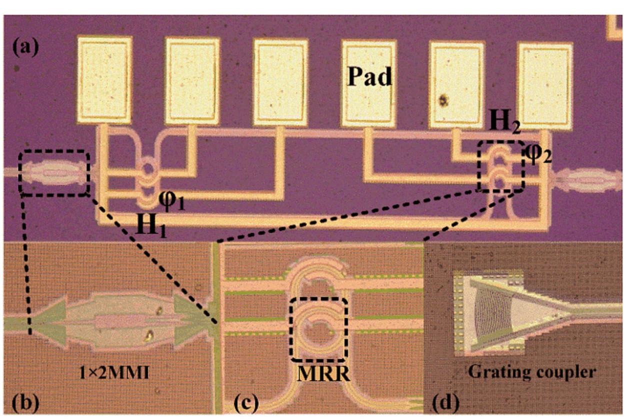

Fig. 5 Optical micrograph **a** tunable bandwidth filter **b** amplifying of the 1 × 2MMI splitter **c** amplifying of the ring resonator with U-bend arm **d** the grating

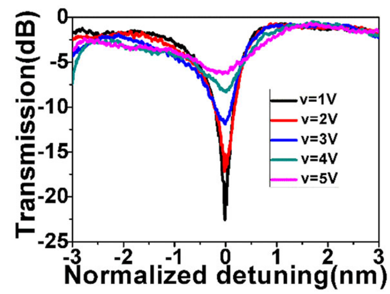

Fig. 6 The spectrum of single MRR with U-bend caused by TO effect

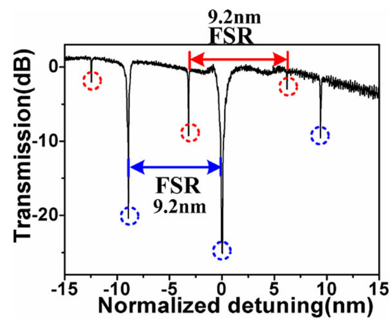

Fig. 7 The spectrum of the device without applying the electric power

The measurements can be obtained by applying the electric power on the heaters of two U-bend waveguides (H_1 and H_2). When the electric power on H_1 is lower than H_2, the bandwidth is broadening toward the larger wavelength similar as red-shift, as shown in Fig. 8a. Figure 8b is the calculated spectra when the extra phase of H_1 is lower than that of H_2. When the electric power on H_1 is higher than H_2, the bandwidth is broadening toward the smaller wavelength similar as blue-shift, as shown in Fig. 8c. Figure 8d is the calculated spectra when the extra phase of H_1 is higher than that of H_2. The phenomenon can be analyzed as follows: when the voltage on H_1 is lower than on H_2, which means the extra phase φ_1 is smaller than φ_2, the extinction ratio in transmission 1 is relatively larger than that in transmission 2, so the waveform broadens toward the smaller extinction ratio of transmission 2 according to Fig. 4 and finally generates the forward Fano-resonance wave. The same analysis is the backward Fano-resonance wave. As is shown in Fig. 8, we can easily find that the bandwidth broadens apparently both in forward and backward waves and all of those shapes agree with theoretical simulations. The largest bandwidth in forward

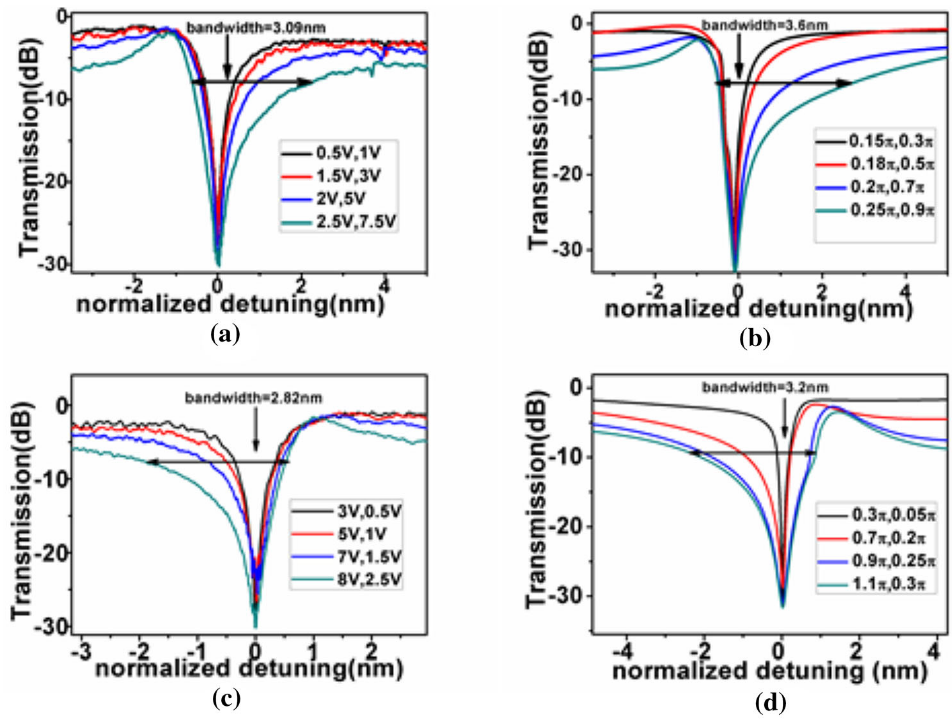

Fig. 8 **a** Measured bandwidth red-shift waveform **b** simulated bandwidth red-shift waveform **c** measured bandwidth blue-shift waveform **d** simulated bandwidth blue-shift waveform (colour figure online)

Fan-resonance shape is 3.09 nm when H_1 is applied on 2.5 V and H_2 is applied on 7.5 V. It is a little smaller than 3.6 nm which is obtained in the simulated spectrum (Fig. 8b). The largest bandwidth in backward Fan-resonance shape is 2.82 nm when H_1 is applied on 8 V and H_2 is applied on 2.5 V. It is also a little smaller than 3 nm which is obtained in the simulated spectrum (Fig. 8d). When there is no voltage on two MRRs, the bandwidth is 0.46 nm. In this scenario, the bandwidth of tunable filter is from 0.46 to 3.09 nm in our experiment, and the extinction ratio is more than 25 dB, which achieving the functions of tunable bandwidth filter.

Conclusion

In conclusion, we demonstrate a bandwidth-tunable optical filter based on microring resonator and MZI with Fano resonance. The device is fabricated on SOI wafer by complementary metal–oxide–semiconductor (CMOS) compatible process. By tuning the phase shifts, we can get bandwidth red-shift and blue-shift. The tunable bandwidth from 0.46 to 3.09 nm is obtained and the extinction ratio is higher than 25 dB. Our wider bandwidth filter can be compatible with SOI platform and apply for high-speed and intensive communication channels. It is also a good candidate for the next generation optical network systems.

Acknowledgements This work is supported by the National Nature Science Foundation of China (NSFC) Nos. (61701441, 61703368), Zhejiang Provincial Natural Science Foundation of China under Grant Nos. (LQ18F030003, LQ17F010001), the Research foundation of Zhejiang provincial department of education (Y201635593).

References

1. J. Cardenas, M.A. Foster et al., Wide-bandwidth continuously tunable optical delay line using silicon microring resonators. Opt. Express **18**(25), 26525–26534 (2010)
2. S.J. Savory et al., Digital coherent optical receivers: algorithms and subsystems. IEEE J. Sel. Top. Quant. **16**(5), 1164–1179 (2010)
3. N. Izhaky, M.T. Morse et al., Development of CMOS-compatible integrated silicon photonics devices. IEEE J. Sel. Top. Quant. **12**(6), 1688–1698 (2006)
4. R. Soref, The past, present, and future of silicon photonics. IEEE J. Sel. Top. Quant. **12**(6), 1678–1687 (2006)

5. J. Tsai, M. Wu et al., 1 $\times$ N^2 wavelength-selective switch with two cross-scanning one-axis analog micromirror arrays in a 4-f optical system. J. Lightwave Technol. **24**(2), 897–903 (2006)
6. S. Frisken, G. Baxter, et al. Flexible and grid-less wavelength selective switch using LCOS technology. *OSA Proc. OFC/NFOEC, OTuM3*, 1–3 (2011)
7. L.J. Zhou, A.W. Poon et al., Fano resonance-based electrically reconfigurable add–drop filters in silicon microring resonator-coupled Mach-Zehnder interferometers. Opt. Express **32**(7), 781–783 (2007)
8. X. Wang, W. Shi et al., Narrow-band waveguide Bragg gratings on SOI wafers with CMOS-compatible fabrication process. Opt. Express **20**(14), 15547–15558 (2012)
9. P. Orlandi, C. Ferrari et al., Reconfigurable silicon filter with continuous bandwidth tunability. Opt. Express **37**(17), 3669–3671 (2012)
10. H. Shen, M.H. Khan et al., Eight-channel reconfigurable microring filters with tunable frequency, extinction ratio and bandwidth. Opt. Express **18**(17), 18067–18076 (2010)
11. M.S. Dahlem, C.W. Holzwarth et al., Reconfigurable multi-channel second-order silicon microring-resonator filterbanks for on-chip WDM systems. Opt. Express **19**(1), 306–316 (2011)
12. L. Ying, X.Y. Fu et al., Fano resonance and spectral compression in a ring resonator drop filter with feedback. Opt. Express **284**(1), 476–479 (2011)
13. L. Chen, N. Sherwood-Droz et al., Compact bandwidth-tunable microring resonators. Opt. Letter **32**(22), 3361–3363 (2007)
14. Y.H. Ding, M.H. Pu et al., Bandwidth and wavelength-tunable optical bandpass filter based on silicon microring-MZI structure. Opt. Express **19**(7), 6462–6470 (2011)
15. T. Hirooka, M. Nakazawa et al., Bright and dark 40 GHz parabolic pulse generation using a picosecond optical pulse train and an arrayed waveguide grating. Opt. Lett. **33**(10), 1102–1104 (2008)
16. G. Zhao, T. Zhao et al., Tunable Fano resonances based on microring resonator with feedback coupled waveguide. Opt. Express **24**(18), 20187–20195 (2016)

Publisher's Note Springer Nature remains neutral with regard to jurisdictional claims in published maps and institutional affiliations.